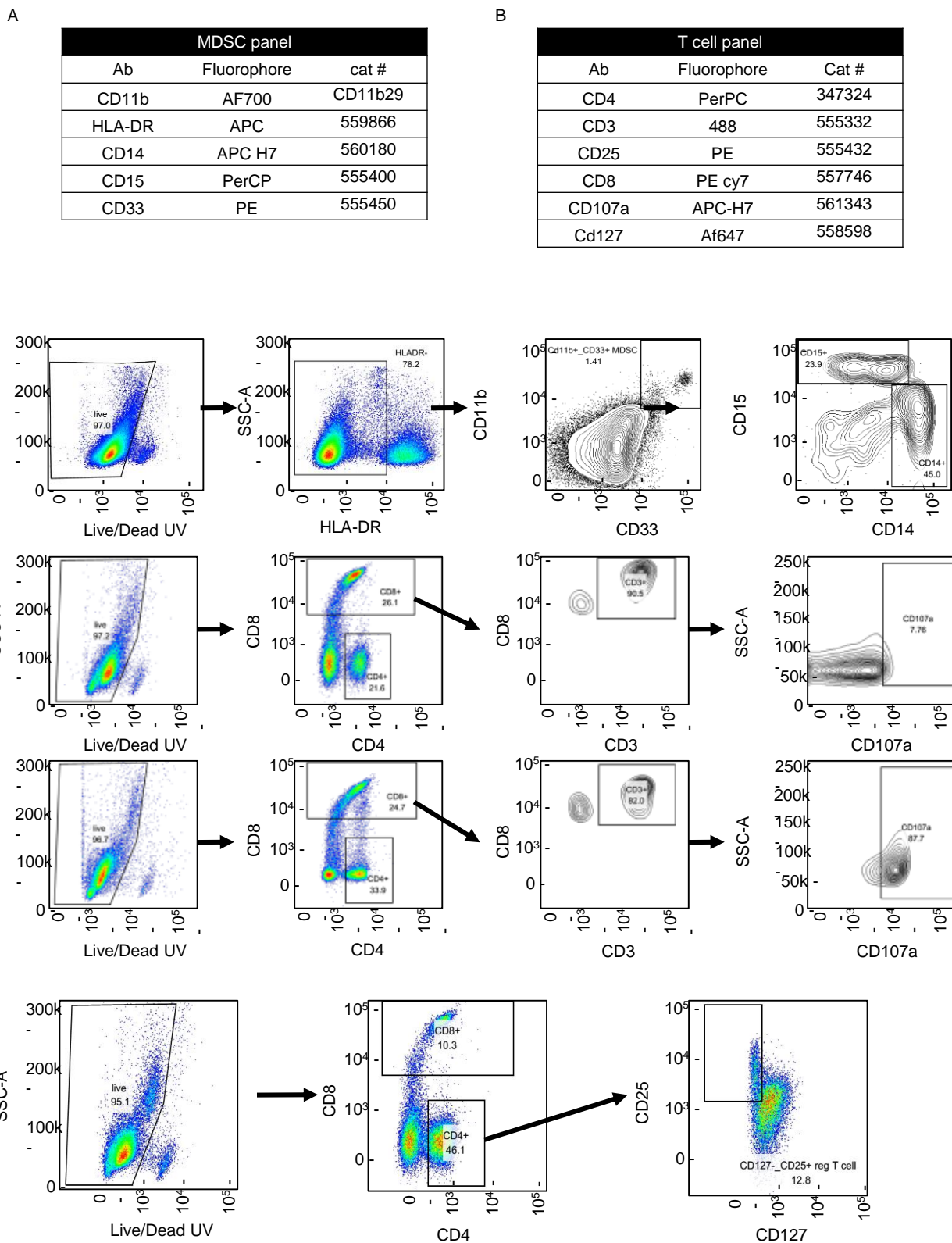
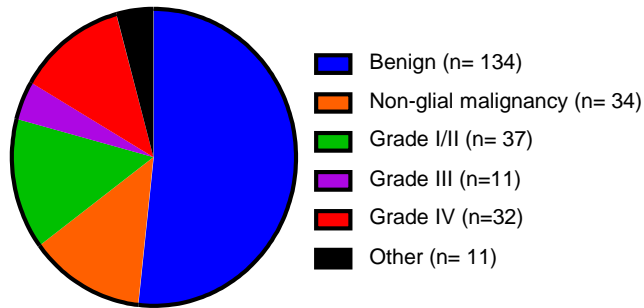


Supplemental Materials

Supplemental Figure 1 Multi-parameter flow cytometry panel and gating strategy



Supplemental Figure 2 Categorizing patient samples for multi-parameter flow cytometry analysis.



Benign (n= 134)

- Meningioma (n= 55)
- Fibroma (n=1)
- Pilocytic Astrocytoma (n=7)
- Pituitary Adenoma (n=49)
- Schwannoma (n=14)
- Choroid Plexus Papiloma (n=1)
- Craniopharyngioma (n=2)
- Gangliocytoma (n=1)
- Hemangioblastoma (n=3)
- LG Glioneuronal Tumor (n=1)

Non-glial malignancy (n= 34)

- Metastasis (n=5)
- Adenoid Cystic Carcinoma (n=1)
- Breast Cancer Met (n= 5)
- Lung Cancer Met (n=9)
- Cervical Met (n=1)
- Esophageal Met (n=2)
- Lymphoma (n=3)
- Myeloma (n=1)
- Chondrosarcoma (n=1)
- Embryol Tumor Grade IV (n=1)
- Metastatic Neuroendocrine Carcinoma (n=1)
- Plasma cell Neoplasm (n=1)
- Recurrent HG Sarcoma (n= 1)
- Renal Cell Carcinoma (n=1)
- Small B cell Neoplasm (n=1)

Grade I/II (n= 37)

- Astrocytoma Grade I (n=2)
- Astrocytoma Grade II (n=9)
- Ependymoma (n=4)
- Glioma Grade I (n=14)
- Glioma Grade II (n= 1)
- Oligoastrocytoma (n=1)
- Oligodendroglioma Grade I (n=2)
- Oligodendroglioma Grade II (n= 4)

Grade III (n=11)

- Anaplastic Oligodendroglioma (n= 1)
- Anaplastic Astrocytoma (n=8)
- Meningioma (n=1)
- Ganglioma (n=1)

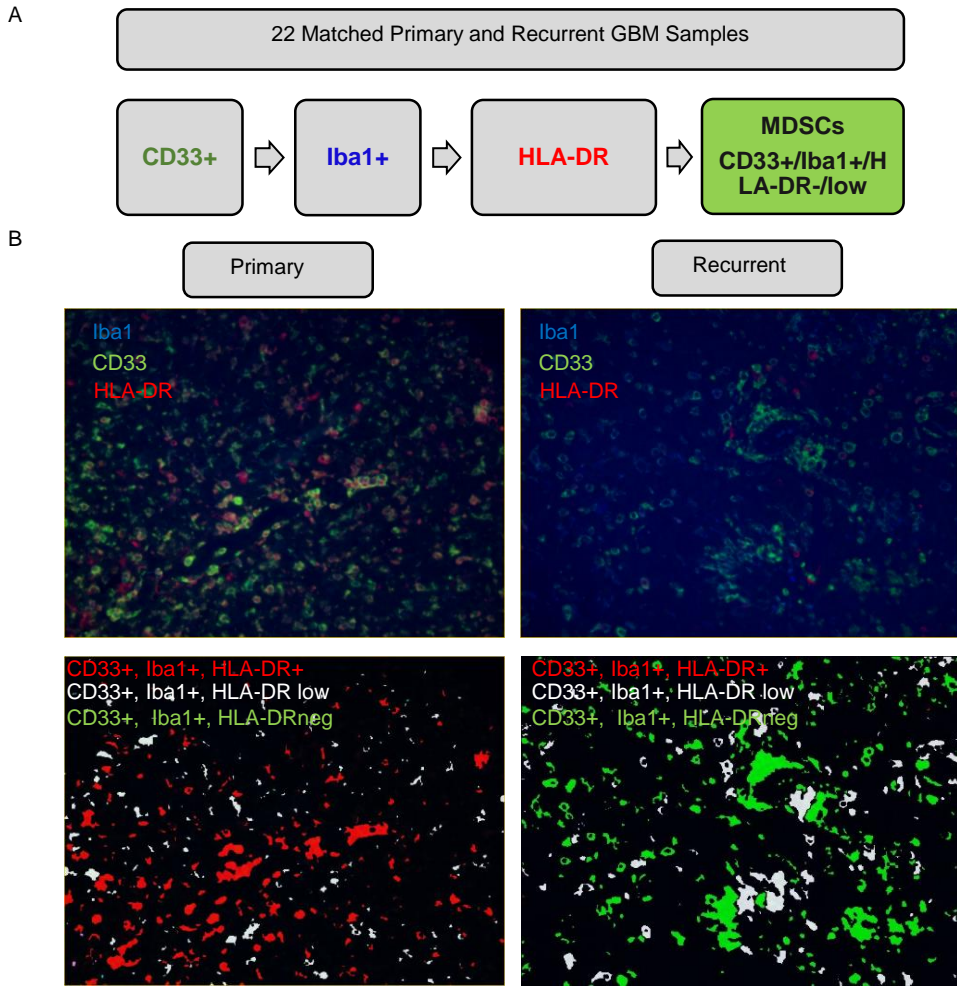
Grade IV (n=32)

- Glioblastoma (n=32)

Other (n= 11)

- Abscess (n=1)
- Cholesterol Granuloma (n=1)
- Cyst (n=1)
- Epidermoid Cyst (n=1)
- Gliosis (n=1)
- Non-neoplastic, Gliosis (n=1)
- Gliosis and Myelin loss (n=1)
- May represent a Rathke cleft cyst (n=1)
- Necrosis (n=1)
- Pituitary inflammatory cyst (n=1)
- Rathke Cleft Cyst (n=1)

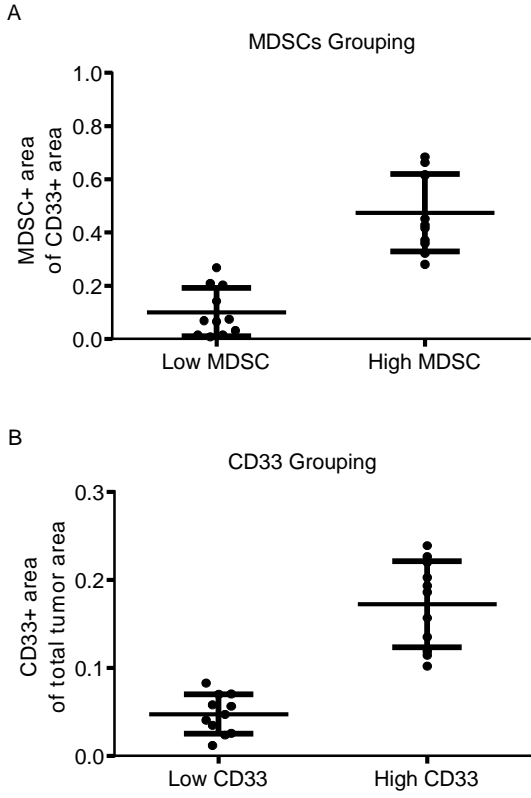
Supplemental Figure 3 Representative image of MDSC staining for one patient who had low MDSCs at primary resection and increased levels upon recurrence.



C

Patient Characteristics (n=22)		
Age at presentation (mean, SD)		60.6 (10.5)
Sex, Male		10 (45%)
Race, Non-Hispanic White		22 (100%)
BMI at presentation (mean, SD)		26.5 (4.5)
Obese at presentation		3 (15%)
Comorbidities		
CHF		(0%)
Peripheral vascular disease		(0%)
Hypertension		5 (23%)
Diabetes mellitus		(0%)
Hypothyroidism		1 (5%)
HIV/AIDS		(0%)
Lymphoma		(0%)
Rheumatoid arthritis, collagen vascular disease		1 (5%)
Alcohol abuse		1 (5%)
Drug abuse		1 (5%)
Tobacco use		(0%)
Ex-smoker		7 (32%)
Current smoker		4 (18%)
Never smoker		11 (50%)

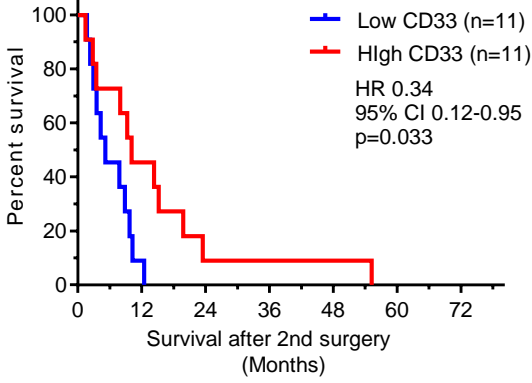
Supplemental Figure 4 Immunofluorescence staining of MDSCs and myeloid cells in matched GBM resections



Supplemental Figure 5 Kaplan–Meier survival analysis of significant survival differences indicated in Table 2

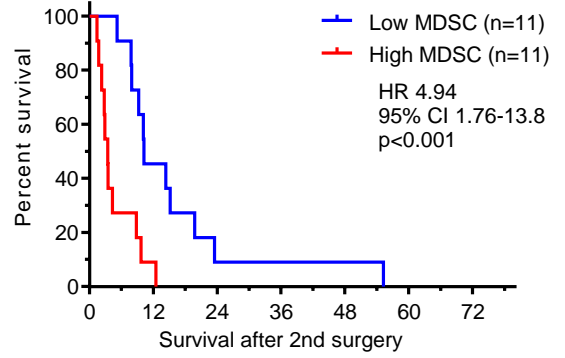
A

Recurrent CD33 Survival after 2nd surgery



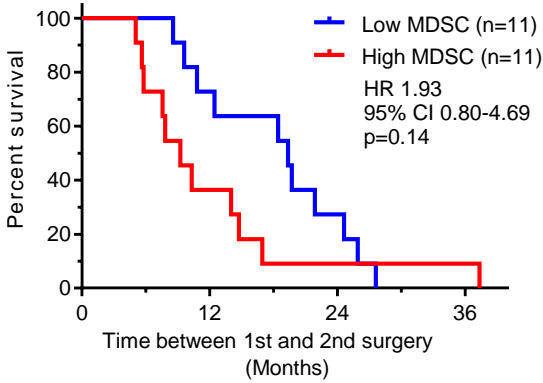
B

Recurrent MDSC in CD33 survival after 2nd surgery



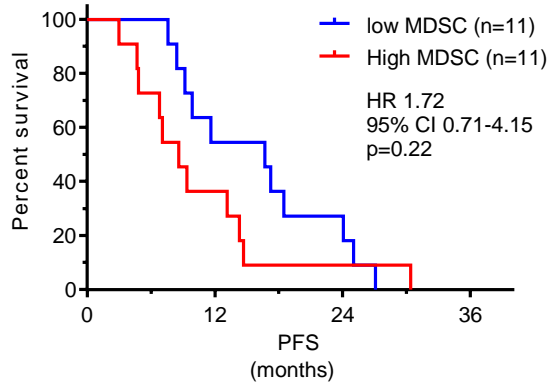
C

Recurrent MDSC in CD33 time between surgeries

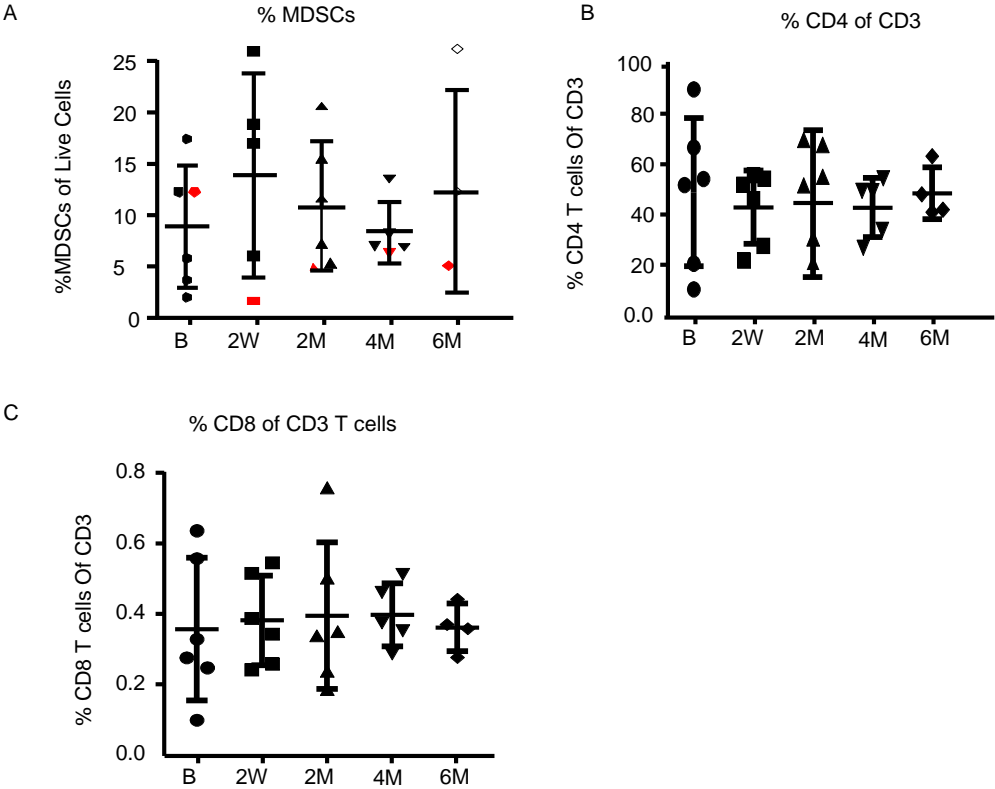


D

Recurrent MDSC in PFS



Supplemental Figure 6 Longitudinal study of 6 newly diagnosed glioblastoma patients for MDSC and T cell levels.



Supplemental Figure 7 CyTOF study using 25 markers to identify immune cell populations that change over time.

A B

label	signal di	target	Clone #	Cat #
209Bi	226	CD11b (Mac-1)	ICRF44	3209003B
170Er	590	CD3	UCHT1	3170001B
167Er	204	CD27	L128	3167006B
165Ho	1000	CD61	VI-PL2	3165010B
164Dy	133	CD15 (SSEA-1)	W6D3	3164001B
163Dy	60	CD56 (NCAM)	NCAM16.2	3163007B
146Nd	508	CD8a	RPA-T8	3146001B
159Tb	500	CD11c	Bu15	3159001B
158Gd	142	CD33	WM53	3158001B
169Tm	100	CD45R A	HI100	3169008B
89Y	800	CD45	HI30V	3089003B
153Eu	290	CD7	CD7-6B7	3153014B
151Eu	150	CD14	M5E2	3151009B
150Nd	70	CD161	HP-3G10	3159004B
149Sm	333	CD66a	CD66a-B1.1	3149008B
148Nd	70	CD16	3G8	3148004B
147Sm	300	CD20	2H7	3147001B
145Nd	70	CD4	RPA-T4	3145001B
143Nd	575	CD25 (IL-2R)	2A3	3149010B
142Nd	232	CD19	HIB19	3142001B
141Pr	216	CD196 (CCR6)	11A9	3141014A
139La	1000	CD107a (LAMP1)	H4A3	3151002B
174Yb	3000	HLA-DR	L243	3174001B
155Gd	167	CD279 (PD-1)	EH12.2H7	3155009B
176Yb	200	CD127 (IL-7Ra)	A019D5	3176004B

PMN-MDSCs (minimum CD45+, CD66a-, CD3-, CD19-, CD20-, CD56-, CD14-, CD11b+, CD15+) (better CD45+, CD66a-, CD3-, CD19-, CD56-, HLADR^{low/-}, CD11b+, CD33+, CD14-, CD15+)

M-MDSCs (CD45+, CD66a-, CD3-, CD19-, CD20-, CD56-, HLADR^{low/-}, CD11b+, CD33+, CD14+, CD15-)

e-MDSCs (CD45+, CD66a-, CD3-, CD19-, CD20-, CD56-, HLADR-, CD33+)

Classical monocytes (CD45+, CD66a-, CD3-, CD19-, CD20-, CD56-, CD14^{high}, CD16-, HLA-DR+)

Intermediate monocytes (CD45+, CD66a-, CD3-, CD19-, CD20-, CD56-, CD14^{high}, CD16+)

Non-classical monocytes (CD45+, CD66a-, CD3-, CD19-, CD20-, CD56-, CD14^{low/+}, CD16+)

Myeloid dendritic cells (CD45+, CD66a-, CD3-, CD19-, CD20-, CD56-, CD14-, CD11b+, CD11c+, HLA-DR+)

Monocyte-derived dendritic cells (CD45+, CD66a-, CD3-, CD19-, CD20-, CD56-, CD14+, CD11b+, CD11c+, HLA-DR+)

Natural killer cells 1 (CD45+, CD66a-, CD3-, CD19-, CD20-, CD14-, CD11c-, CD56-, CD16+)

Natural killer cells 2 (CD45+, CD66a-, CD3-, CD19-, CD20-, CD14-, CD11c-, CD56+, CD16-)

Granulocytes (CD3-, CD20-, CD14-, CD11c-, CD45-, CD66a+)

Naïve CD8+ T cells (CD45+, CD66a-, CD3+, CD8a+, CD45RA+, CD27+, CD127+)

Effector T killer cells (CD45+, CD66a-, CD3+, CD8a+, CD45RA+, CD27-)

Activated T killer cells (CD45+, CD66a-, CD3+, CD8a+, HLA-DR+)

Cytotoxic T cells (CD45+, CD66a-, CD3+, CD8a+, CD107a+)

Memory T killer cells (CD45+, CD66a-, CD3+, CD8a+, CD45RA-, CD27+)

DP T cells (CD45+, CD66a-, CD3+, CD8a+, CD4+, CD27+, CD161+)

Naïve CD4+ T cells (CD45+, CD66a-, CD3+, CD4+, CD45RA+, CD25-, CD127+, CD27+)

Activated T helper cells (CD45+, CD66a-, CD3+, CD4+, HLA-DR+)

Effector T helper cell (CD45+, CD66a-, CD3+, CD4+, CD45RA+/-, CD25+, CD127-, CD27-)

Effector regulatory T helper cells (CD45+, CD66a-, CD3+, CD4+, CD45RA-, CD25+, CD127-)

Resting regulatory T helper cells (CD45+, CD66a-, CD3+, CD4+, CD45RA+, CD25+, CD127-)

Memory T helper cells (CD45+, CD66a-, CD3+, CD4+, CD45RA-, CD25+, CD127+, CD27+)

Th17 cells (CD45+, CD66a-, CD3+, CD4+, CD161+, CD196+)

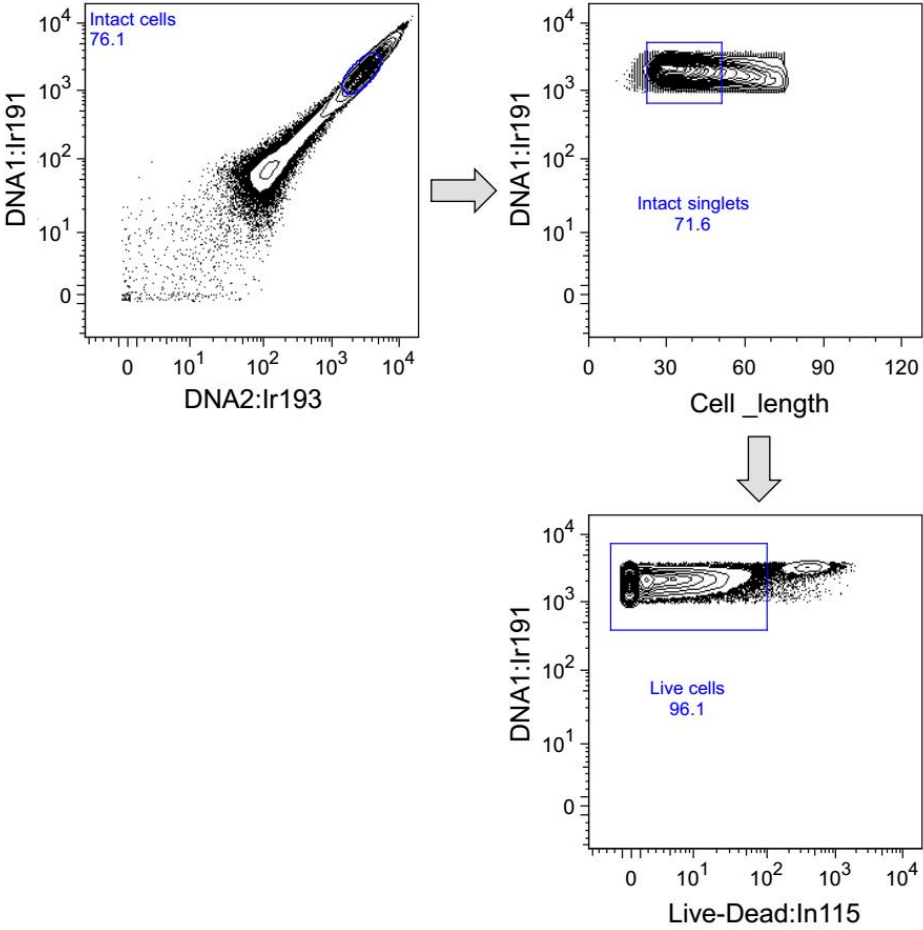
Naïve B cells (CD45+, CD66a-, CD3-, CD19+, CD20+, HLA-DR+, CD27-)

Plasma B cells (CD45+, CD66a-, CD3-, CD19+, CD20-, HLA-DR-, CD27+)

Memory B cells (CD45+, CD66a-, CD3-, CD19+, CD20+, HLA-DR+, CD27+, CD196+)

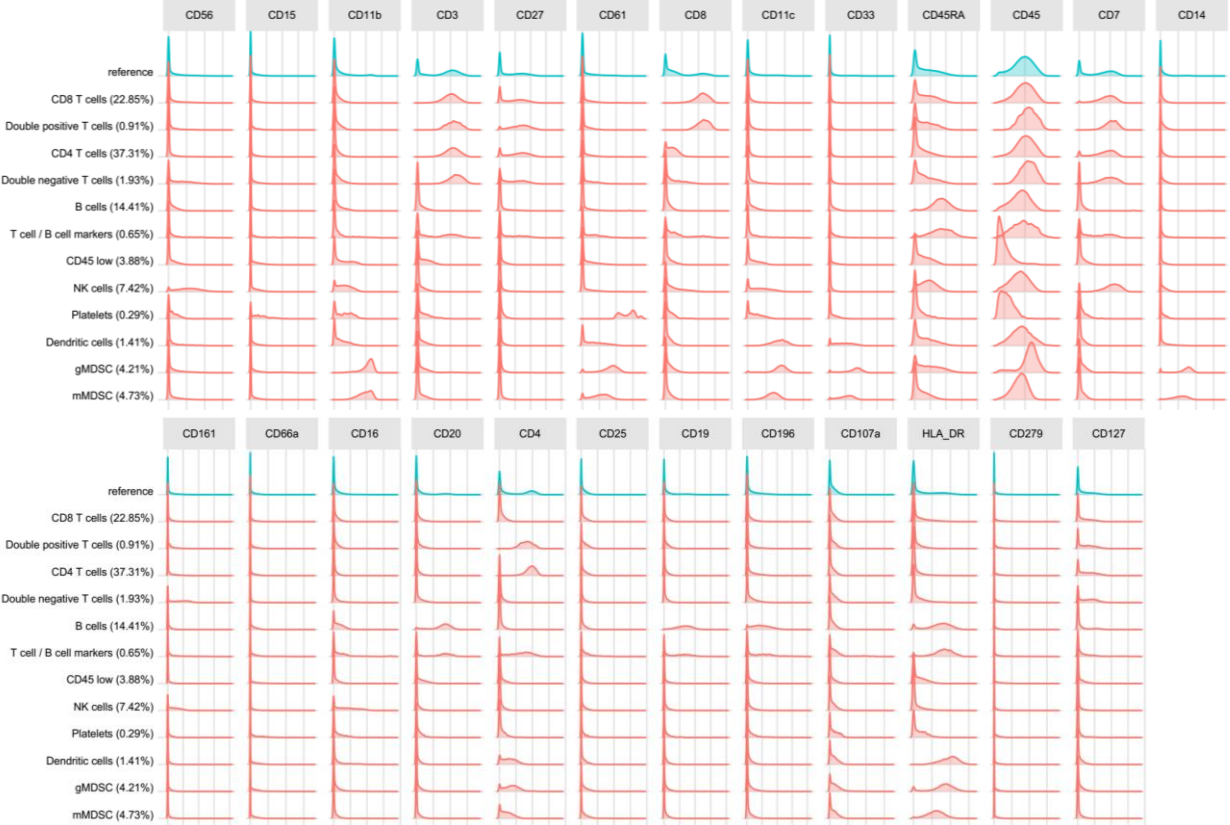
Platelets (CD45-, CD61+)

Supplemental Figure 8 CyTOF cleaning gates was performed to choose live single cells for analysis.



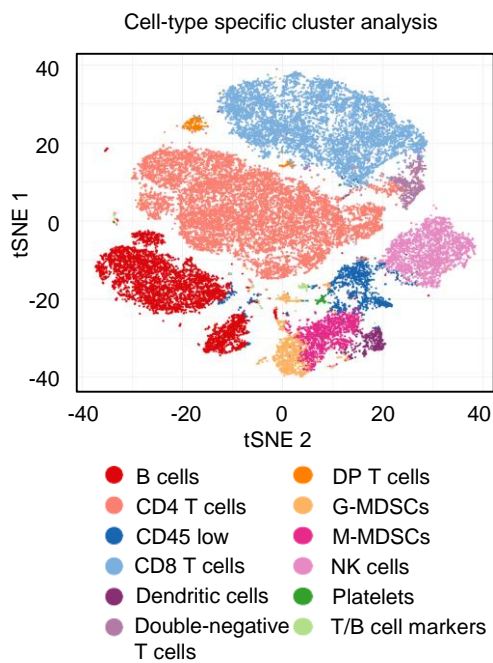
Supplemental Figure 9 tSNE cluster analysis of 30 clusters via histogram for expression of each marker is an unbiased approach to identify cell populations

Defining clusters GBM timepoints

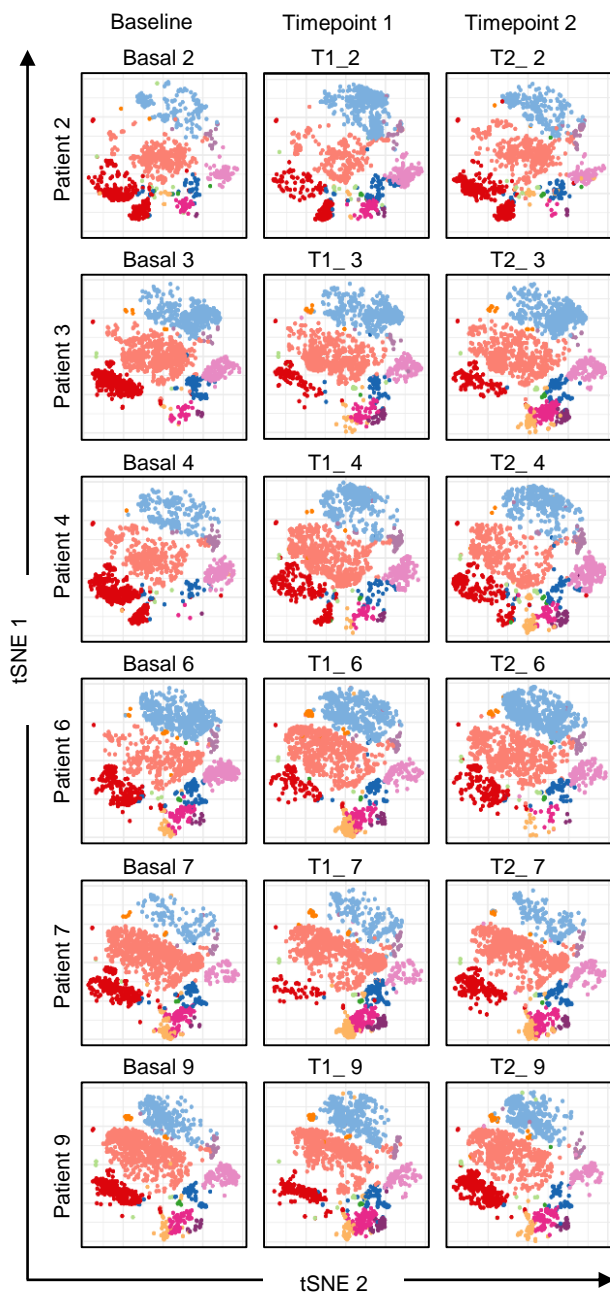


Supplemental Figure 10 tSNE plots identify immune shifts over time in GBM patients

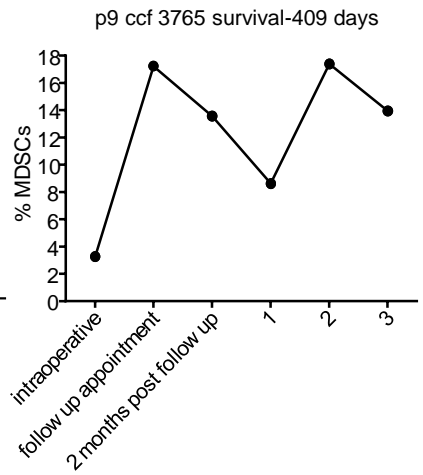
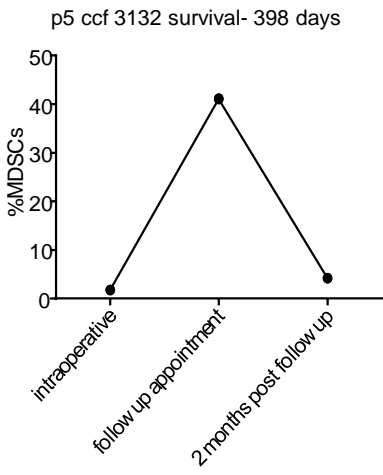
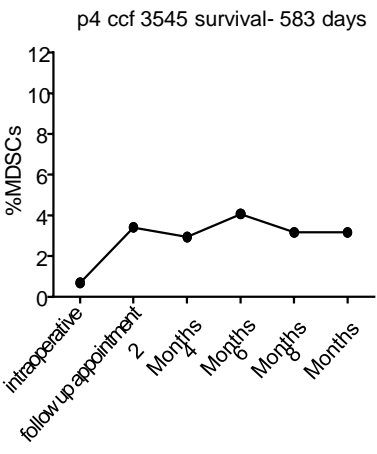
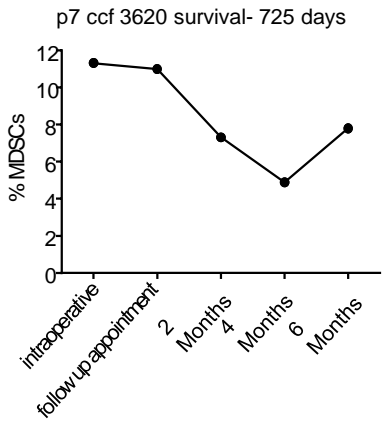
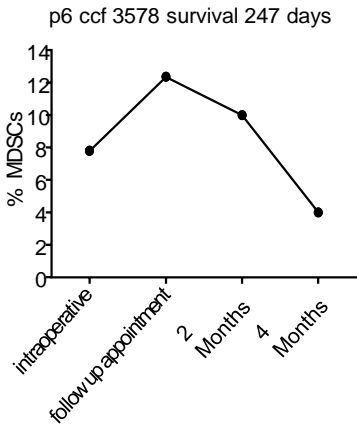
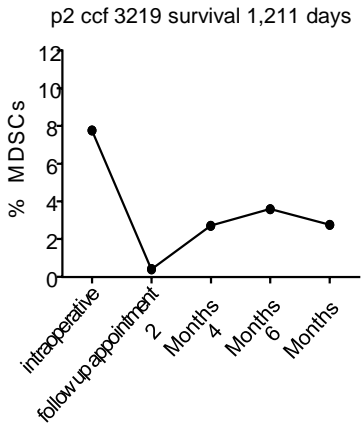
A



B

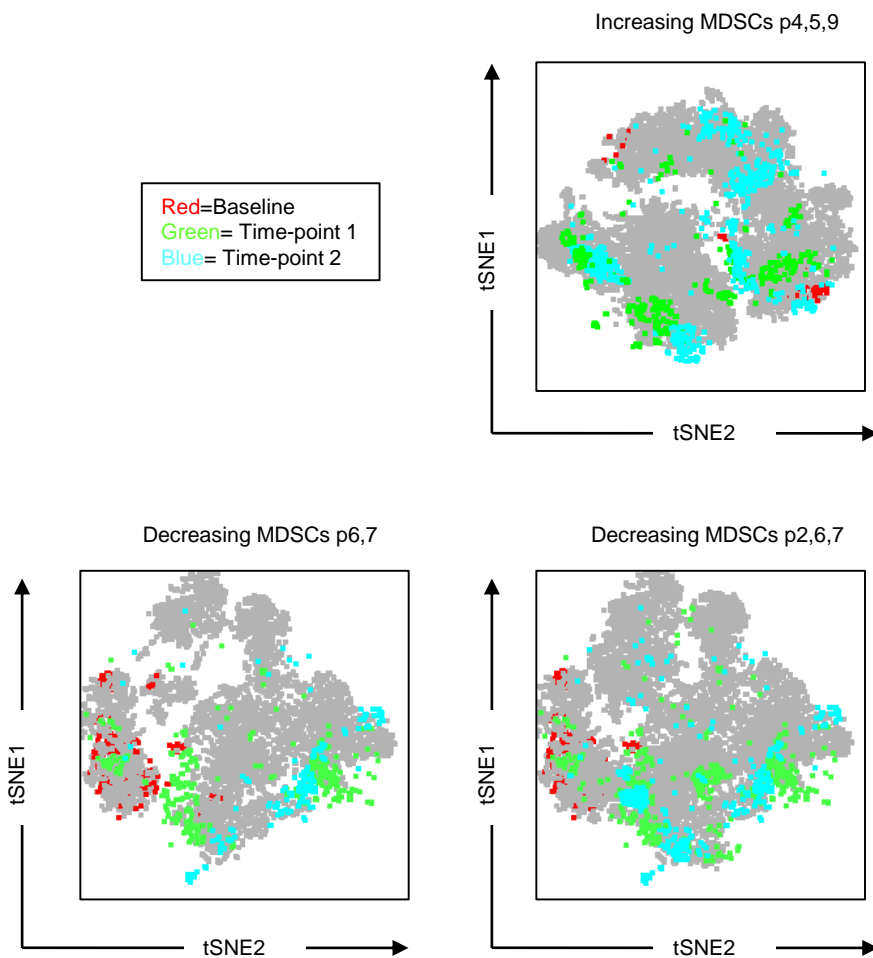


Supplemental Figure 11 Of 6 newly diagnosed GBM patients 3 had a good prognosis and decreasing MDSC while 3 had a poor prognosis and increasing MDSCs

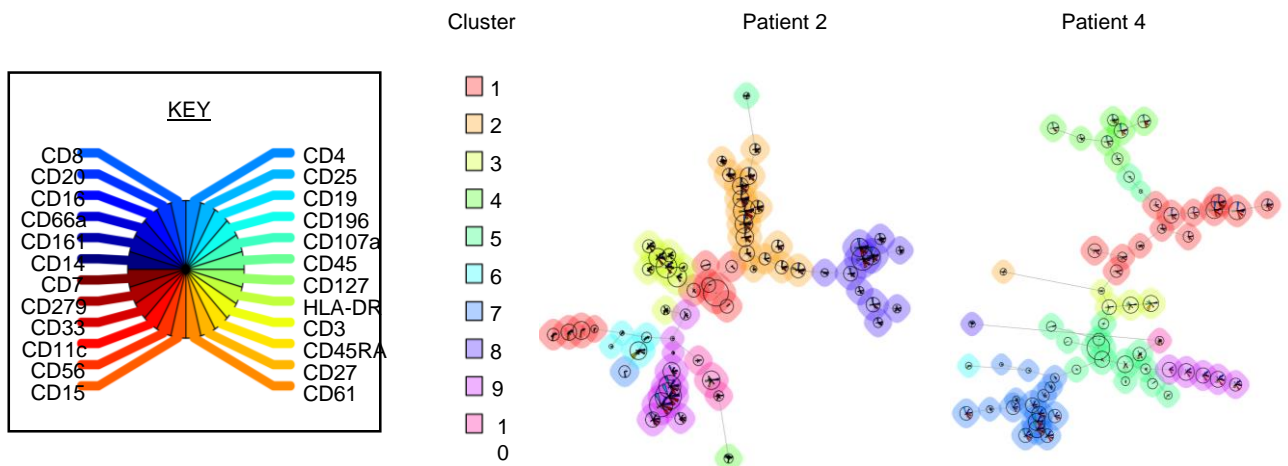


Supplemental Figure 12 IDH1 mutant GBM patient has similar MDSCs changes over time compared to WT patients with a good prognosis, but a distinct immune landscape from those with a poor prognosis

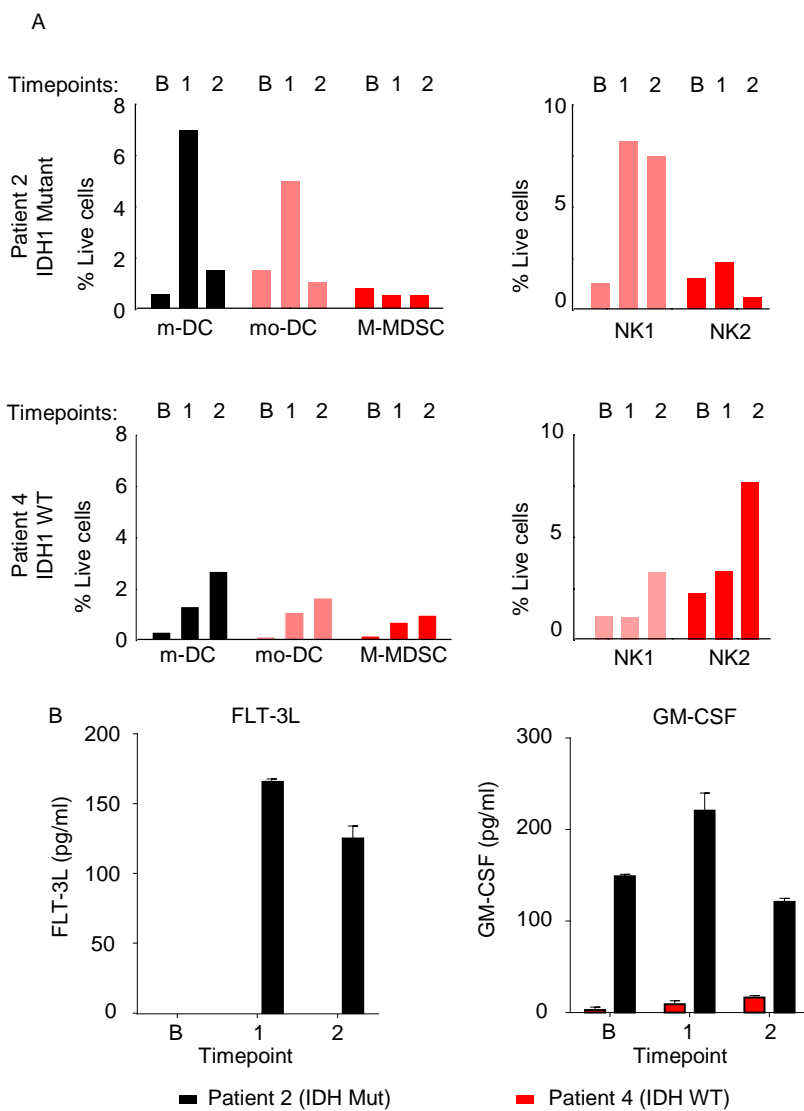
A



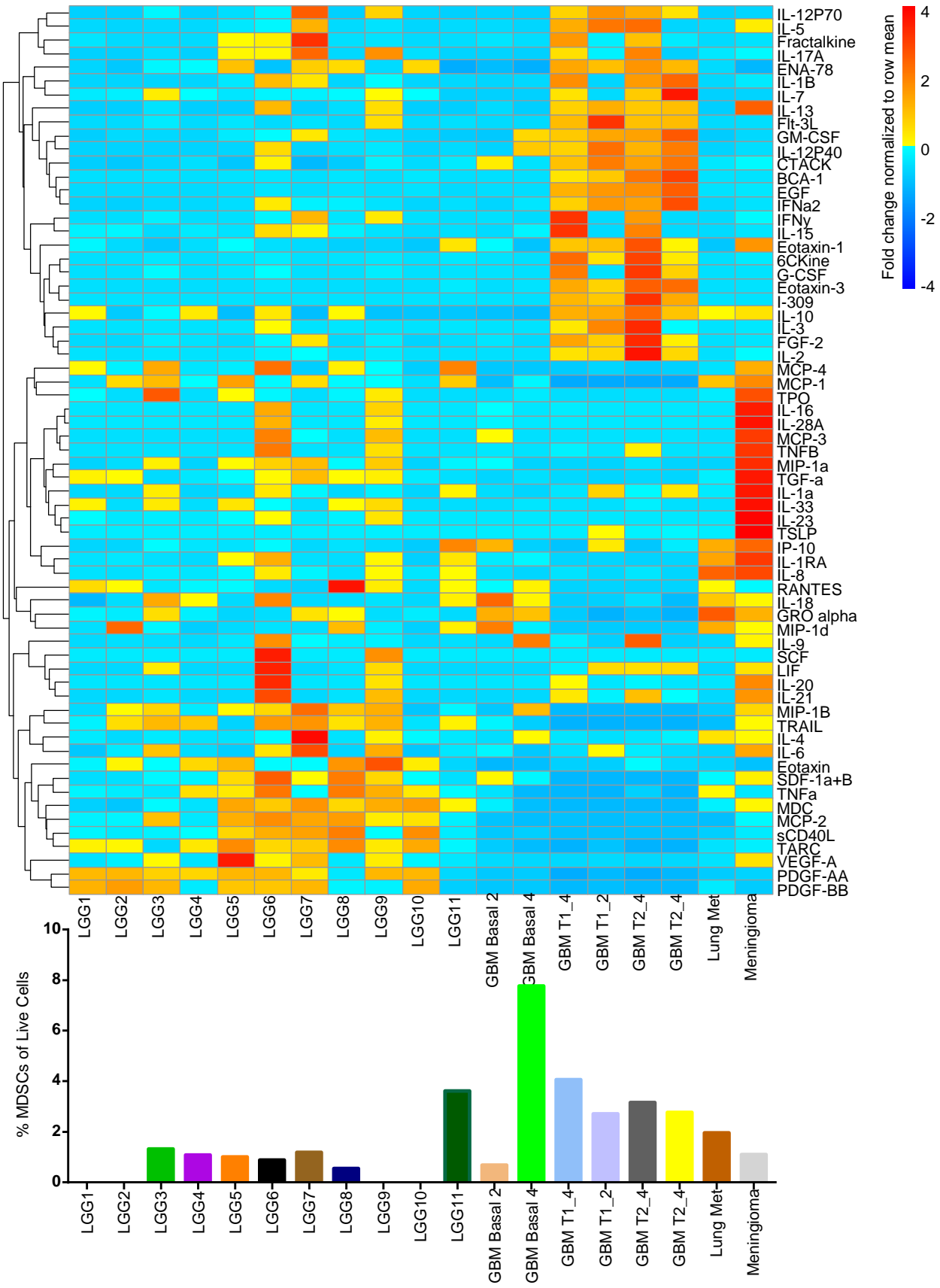
B



Supplemental Figure 13 Dendritic cells and antigen-presenting cells are increased in a patient with a good prognosis



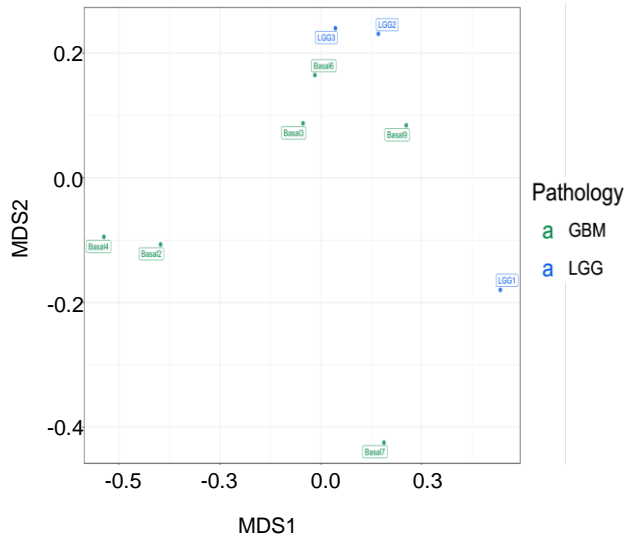
Supplemental Figure 14 Cytokine array of glioblastoma and low-grade glioma patients identifies a unique cytokine signature for glioblastoma patients as they progress through disease LGG vs GBM



Supplemental Figure 15 . tSNE analysis of LGG and GBM samples at baseline allows for a visual identification of immune shifts

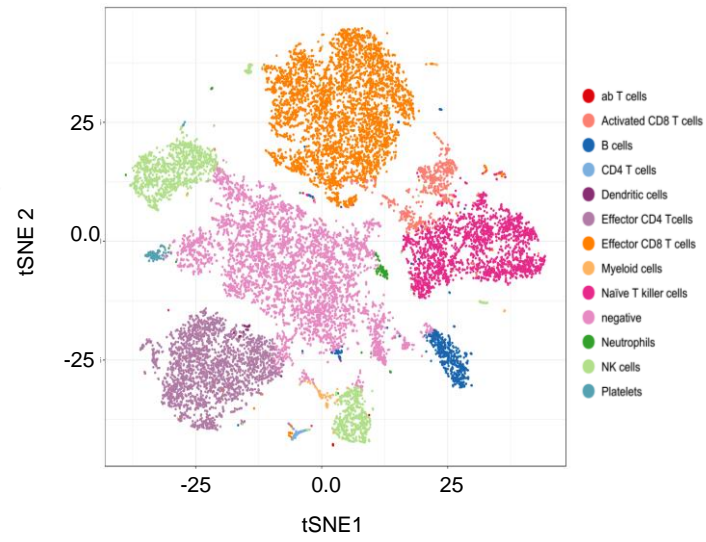
A

GBM and LGG MDS analysis

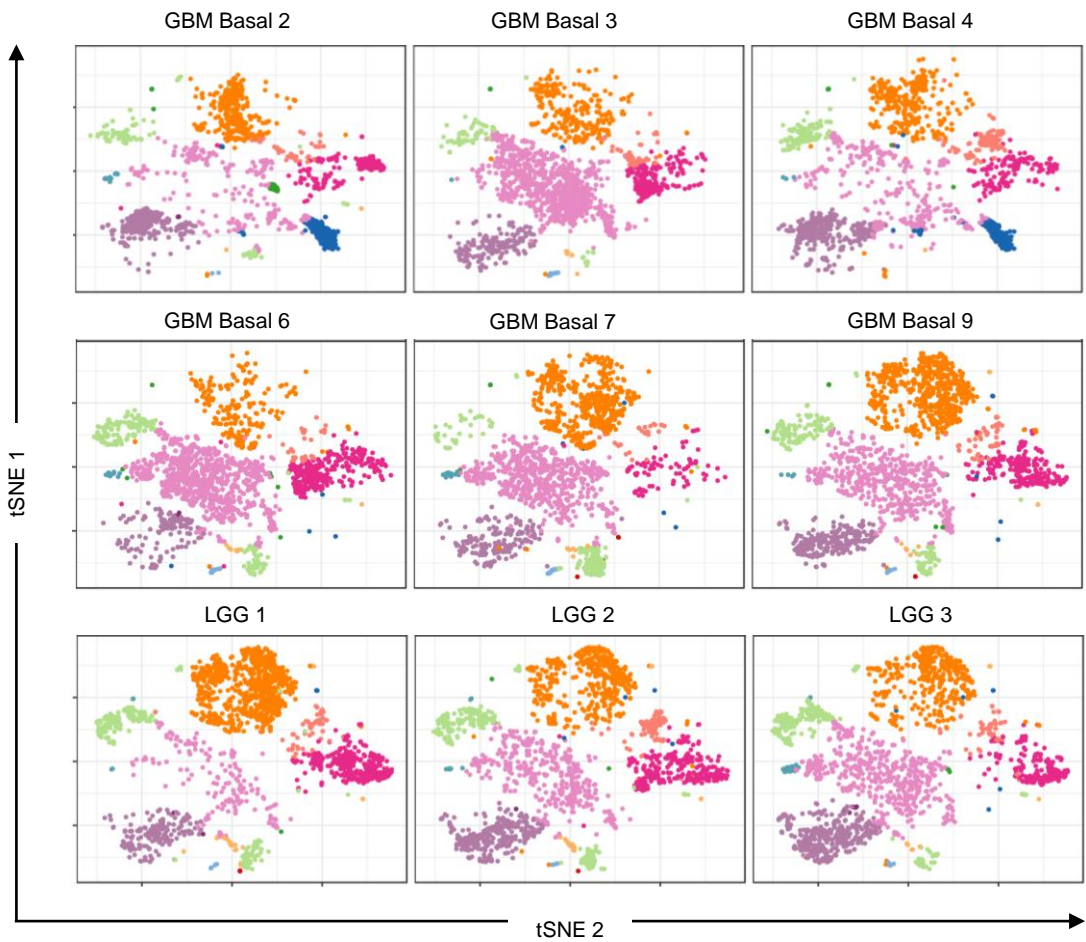


B

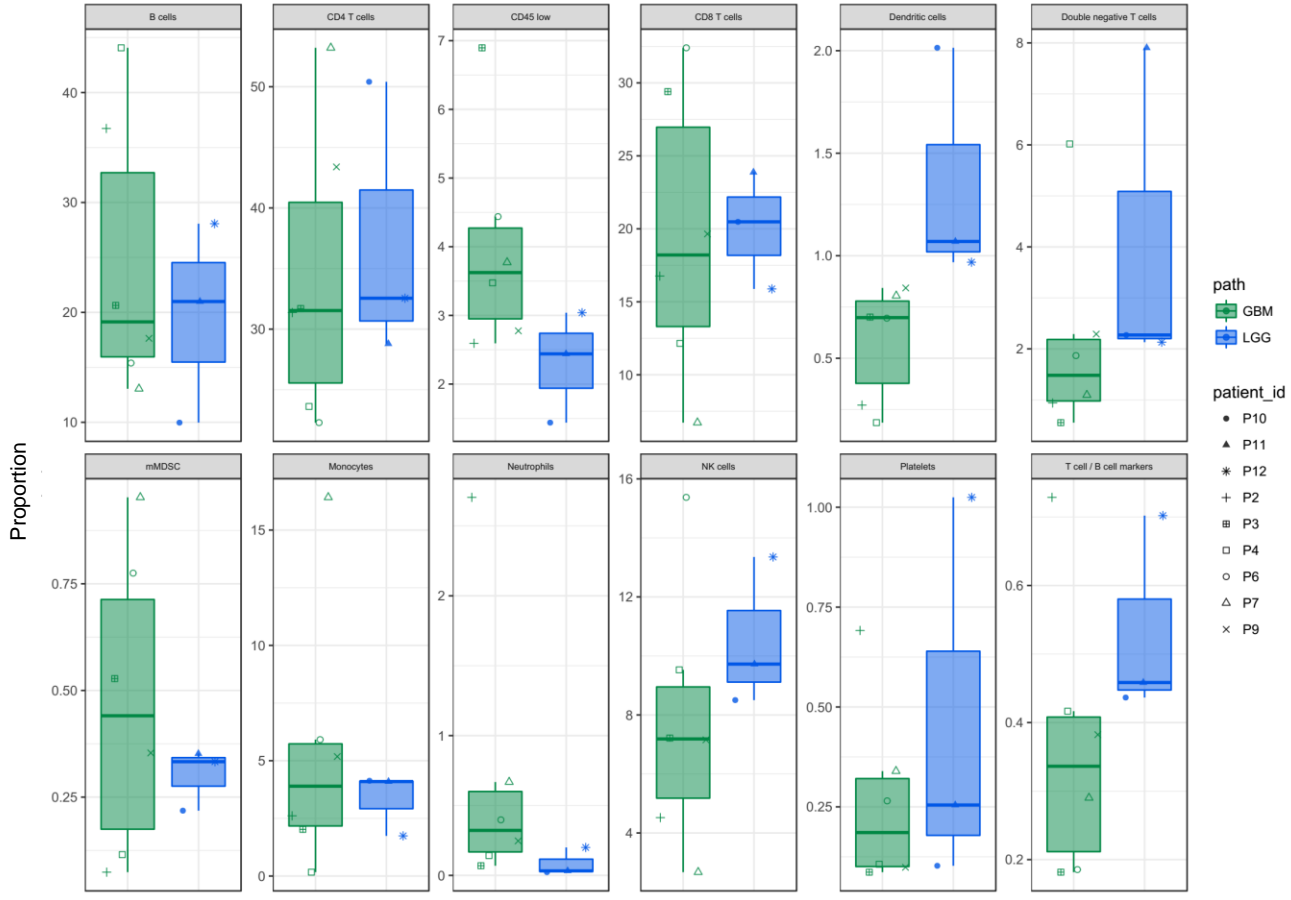
GBM and LGG tSNE analysis



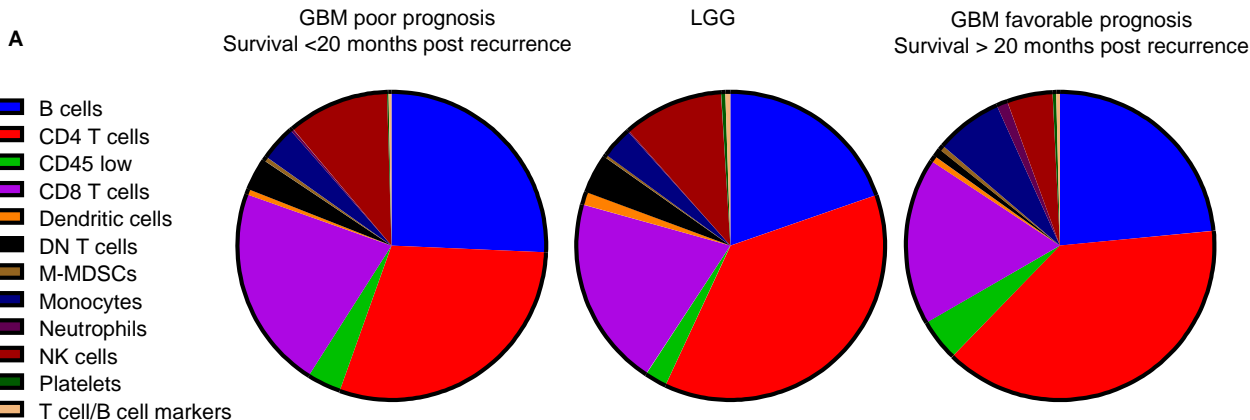
C



Supplemental Figure 16 CyTOF analysis comparing six GBM patients and three LGG patients identifies significant differences in immune status.
Cluster Defining LGG vs GBM



Supplemental Figure 17 Comparing GBM patients with varying prognoses to LGG patients identifies shifts in immune cell populations.



Supplemental Table 1 Cox regression analysis of MDSCs with Age, MGMT, Sex, and steroid use taken into account identify MDSCs as the most significant variable in the model.

Cox Regression analysis MDSCs

Variable	No of patients	HR (95% CI)	P value
Age [#] (continuous)	22	1.04 (0.98-1.11)	0.22
MGMT promoter status			
Methylated	9	1.00	
Unmethylated	13	11.01 (2.18-55.61)	0.004
Sex			
Male	10	1.00	
Female	12	0.65 (0.21-1.97)	0.45
Steroid use ^{##}			
Yes	13	1.00	
No	9	0.51 (0.18-1.48)	0.22
MDSC			
Low	11	1.00	
High	11	6.78 (1.89-24.37)	0.003

[#] Age at time of primary diagnosis

^{##} Steroid use is defined as chronic use (>7 days) prior to secondary surgery.

IDH1 status is not included in the analysis, as only one patient in the cohort had a tumor with a R132 IDH1 mutation.

Supplemental Table 2 Cox regression analysis of CD33+ cells with Age, MGMT, Sex, and steroid use taken into account identify CD33+ cells as the most significant variable in the model.

Cox Regression analysis CD33 Myeloid cells

Variable	No of patients	HR (95% CI)	P value
Age [#] (continuous)	22	1.07 (1.00-1.13)	0.043
MGMT promoter status			
Methylated	9	1.00	
Unmethylated	13	10.05 (2.08-48.64)	0.004
Sex			
Male	10	1.00	
Female	12	0.53 (0.17-1.64)	0.27
Steroid use ^{##}			
Yes	13	1.00	
No	9	0.45 (0.15-1.34)	0.15
CD33			
Low	11	1.00	
High	11	0.12 (0.028-0.54)	0.006

[#] Age at time of primary diagnosis

^{##} Steroid use is defined as chronic use (>7 days) prior to secondary surgery.

IDH1 status is not included in the analysis, as only one patient in the cohort had a tumor with a R132 IDH1 mutation.

Supplemental Figure Legends

Supplemental Figure 1. Multi-parameter flow cytometry panel and gating strategy. (A) Multi-parameter flow cytometry analysis of myeloid cells and MDSCs stained with the antibodies and fluorophores listed and analyzed on a BD LSRFortessa™ cell analyzer. (B) Each sample was run through a T cell panel to determine lymphoid cell population quantities using the BD LSRFortessa™. (C) Schematic depicting the gating strategy for MDSCs (live, HLA-DR-/low, CD33, IBA1+), where CD15⁺ cells are considered granulocytic and CD14⁺ are monocytic MDSCs. (D) Analysis of the lymphoid panel with T cell markers distinguishes CD8⁺ T cells as inactivated (top row, CD107a-) or activated (bottom row, CD107a⁺). (E) T regulatory cells are distinguished as CD4⁺ cells that are CD127⁻ and CD25⁺.

Supplemental Figure 2. Categorizing patient samples for multi-parameter flow cytometry analysis. Pie chart from Figure 1 depicts the categories of patient samples: benign, non-glioma malignancy, glioma grade I/II, glioma grade III, glioma grade IV, and other. Below the pie chart, each category is broken down into the pathological diagnoses with the number of each listed to the right.

Supplemental Figure 3. Representative image of MDSC staining for one patient who had low MDSCs at primary resection and increased levels upon recurrence. (A) Schematic representation of the experimental design outlining patients (n=22) with matched primary and secondary resections triple-stained for CD33, Iba1, and HLA-DR to identify MDSCs. (B) Representative images of a patient's primary (left column) and recurrent (right column) samples where MDSCs were increased in the recurrent specimen (identified by green masking in left and right panels). (C) Clinical characteristics of the cohort of the 22 patients with matched primary and secondary tissue samples.

Supplemental Figure 4. Immunofluorescence staining of MDSCs and myeloid cells in matched GBM resections. (A) MDSC grouping from patients (n=22) was divided by the median area of MDSCs in the total tumor area, which was used for Kaplan–Meier survival analysis. (B) As a comparison, CD33⁺ myeloid cells were analyzed in a similar fashion where high and low groups were defined by their median levels in the recurrent tissue. Data is represented as mean and standard deviation.

Supplemental Figure 5. Kaplan–Meier survival analysis of significant survival differences indicated in Table 2. Analysis of immunofluorescence staining of n=22 matched primary and secondary resection GBM patients. High and low groups were identified based on median expression of MDSCs at primary resection and at recurrence (**Table 2**). Here, we have plotted the significant values identified for CD33 levels and MDSC levels, and survival was analyzed after the 2nd surgery (**A, B**). Additionally, MDSC levels, and the time between surgeries and progression free survival are shown (**C, D**).

Supplemental Figure 6. Longitudinal study of 6 newly diagnosed glioblastoma patients for MDSC and T cell levels. (A) Schematic representation of the study design, where samples were collected for n=6 patients over disease progression after being diagnosed with glioblastoma (**B,C,D**) Over disease progression, patients were analyzed at baseline (B), 2 weeks post-op (2W), 2 months post-baseline (2M), and then every following 2 months. One out of six patients were IDH1 Mutant (**red**). Multi-parameter flow cytometry for CD4 T cells (CD3⁺, CD4⁺, CD8⁻), CD8⁺ T cells (CD3⁺, CD4⁻, CD8⁺), CD8⁺ T cells (CD3⁺, CD4⁻, CD8⁺). One-way ANOVA, used to compare

means across timepoints, yielded no significant differences ($p < 0.05$). Data is represented as mean and standard deviation

Supplemental Figure 7. CyTOF study using 25 markers to identify immune cell populations that change over time. (A) A panel of 25 immune markers with heavy metal tags was used to label cell populations. (B) The immune cell populations that are capable of being identified using the 25 markers are listed with their marker selection.

Supplemental Figure 8. CyTOF cleaning gates were performed to choose live single cells for analysis. DNA Ir191/193 was used to mark nucleated cells, which were then further gated for intact cells by length parameters. Next, cells were gated for live/dead In115, where negative cells are live. Cells in this final gate were then subdivided to new FCS files for analysis.

Supplemental Figure 9. tSNE cluster analysis of 30 clusters via histogram for expression of each marker is an unbiased approach to identify cell populations. In the longitudinal study of newly diagnosed patients ($n=6$), 6 patients were analyzed by CyTOF at three timepoints each. tSNE cluster analysis was used to define unique populations of cells. In this analysis, the 6 samples are combined for cluster analysis of each marker, and histograms show the expression level of each marker in the cluster, which were then manually determined to be the immune cell types labeled on the Y axis.

Supplemental Figure 10. tSNE plots identify immune shifts over time in GBM patients. (A) t-distributed stochastic neighbor embedding (tSNE) plot identifies 30 unique populations that are color coded among the patient samples ($n=6$) across all timepoints, representing a total of 18 samples. (B) Individual tSNE plots of each sample demonstrate the quantity of each cell population by density of color-coded clusters over time.

Supplemental Figure 11. Of 6 newly diagnosed GBM patients, 3 had a good prognosis and decreasing MDSC, while 3 had a poor prognosis and increasing MDSCs. Percent MDSCs was assessed by flow cytometry in 6 GBM patients over time, where 3 patients had overall decreasing MDSCs and a good prognosis (top row). The other 3 patients (bottom row) had overall increasing MDSCs over time and a poor prognosis (bottom row).

Supplemental Figure 12. An IDH1-mutant GBM patient has similar MDSC changes over time compared to WT patients with a good prognosis but a distinct immune landscape from those with a poor prognosis. (A) tSNE analysis of the MDSC population from patients with decreasing MDSCs (p2, 6, 7) and increasing MDSCs (p4, 5, 9) was utilized to determine whether inclusion or exclusion of patient 2 (IDH1 mutant) altered the MDSC expression profile over time. In this analysis, removing patient 2 from the analysis did not significantly alter the expression profile of MDSCs (A), and the MDSC profile is still distinctly different between the two groups of patients with differing prognoses. FlowSOM analysis of Patients 2 (IDH1 mutant, good prognosis, decreasing MDSCs) and 4 (IDH1 WT, poor prognosis, increasing MDSCs) creates an unbiased clustering of 10 groups, with each node of the clusters identifying the size of the cell population and pie charts showing their expression of CyTOF markers, demonstrating distinct differences in immune landscape at baseline (B).

Supplemental Figure 13. Dendritic cells and antigen-presenting cells are increased in a patient with a good prognosis. (A) Manual gating of DC populations, M-MDSCs, and NK cells from Patients 2 and 4 at baseline (B), timepoint 1 (1), and timepoint 2 (2), where B and 1 are at the same point in time post-diagnosis and 2 is the final time point collected. (B) Multi-parameter flow cytometry-based cytokine array where the serum levels (in pg/ml) of 65 cytokines were

examined. FLT-3L and GM-CSF were increased in Patient 2 over time. Data is represented as mean and standard deviation

Supplemental figure 14. Cytokine array of GBM and LGG patients identifies a unique cytokine signature for glioblastoma patients as they progress through disease. Heat map representation of the pg/ml of each cytokine on the Y axis, where each row is internally normalized to the highest value. Dendrogram clustering groups the cytokines based on hierarchical clustering. MDSCs of each patient are plotted below their corresponding cytokine levels in the bar chart.

Supplemental Figure 15. tSNE analysis of LGG and GBM samples at baseline allows for a visual identification of immune shifts. (A) Multi-dimensional scaffold analysis of low-grade glioma (LGG) and glioblastoma (GBM) patient samples from CyTOF analysis were compared to determine whether large differences existed between samples based on their grouping within the plot, where similar samples cluster together. (B) Combining CyTOF analysis of six GBM and three LGG patient samples, tSNE analysis was performed to identify unique cell clusters. (C) tSNE analysis of each patient individually is separated to identify immune shifts between GBM and LGG.

Supplemental Figure 16. CyTOF analysis comparing six GBM patients and three LGG patients identifies significant differences in immune status. (A) Unbiased tSNE clustering analysis identifies 12 immune cell populations in n=6 GBM patients at baseline and n=3 LGG patients at baseline. (B) Quantification of the immune cell populations comparing baseline GBM samples to baseline low-grade glioma (LGG) samples identifies significant differences between cohorts for DCs, NK cells, and mixed T-B marker cells. Statistics were determined by comparing baseline to each timepoint using linear models of the data with t-test comparisons and Benjamini-

Hochberg adjust to control for multiple comparisons * $p < 0.05$, ** $p < 0.001$, *** $p < 0.0001$. Graphs represent data sets as median with 1st and 3rd quartiles.

Supplemental Figure 17. Comparing GBM patients with varying prognoses to LGG patients identifies shifts in immune cell populations. (A) Baseline samples from $n=6$ patients in the longitudinal CyTOF study were stratified into three with a good prognosis (p2, 6, 7) and three with a poor prognosis (p4, 5, 9) and compared to $n=3$ LGG patients. These patients were then compared to three low-grade glioma (LGG) patients at baseline using a pie chart with their immune cell populations as defined by tSNE clustering and histogram defining the characteristics.

Supplemental Table 1. Cox regression analysis of MDSCs with age, MGMT status, sex, and steroid use taken into account identifies MDSCs as the most significant variable in the model. As a confirmation of the survival differences seen by log-rank tests in **Figure 1E, F and Table 2**, a Cox regression model was used to test the effect of possible confounding clinical variables. MDSCs remained the most significant predictor of survival ($p=0.003$); $n=22$.

Supplemental Table 2. Cox regression analysis of CD33 with age, MGMT status, sex, and steroid use taken into account identifies CD33⁺ cells as the most significant variable in the model. As a confirmation of the survival differences seen by log-rank tests in **Figure 1E, F and Table 2**, a Cox regression model was used to test the effect of possible confounding clinical variables. CD33⁺ myeloid cells also remained the most significant predictor of survival ($p=0.006$); $n=22$.